

# THE 4TH INTERNATIONAL CONFERENCE ON ALUMINUM ALLOYS

## RECRYSTALLIZATION OF A COMMERCIAL ALUMINUM-IRON-SILICON ALLOY DEFORMED UNDER COLD-WORKING CONDITIONS

E.S. Puchi, C. Villalobos and A. Piñeiro

School of Metallurgical Engineering and Materials Science, Central University of Venezuela, Postal Address 47885, Caracas 1041, Venezuela.

### Abstract

Recrystallization studies on a commercial twin-roll cast aluminum-iron-silicon alloy deformed under cold-working conditions have been carried out by means of restoration of its mechanical properties, optical microscopy, and scanning and transmission electron microscopy techniques. Specimens deformed by cold-rolling to 50% thickness reduction were subsequently annealed at temperatures of 598, 623, 648 and 673 K, which allowed to carry out an analysis of the microstructural evolution and the changes in mechanical properties that take place during the heat treatments applied. The microstructural evolution of this material have been analyzed in terms of the Johnson-Mehl-Avramy-Kolmogorov (JMAK) relationship applied to the restoration data. It has been determined that precipitation reactions concerning small second phase particles tend to occur during the annealing of the material at low temperatures during relatively long periods of time, which gives place to a marked decrease of the recrystallization kinetics and to a significant increase of the activation energy of the restoration processes.

### Introduction

The industrial processing of commercial twin-roll cast (TRC) aluminum-iron-silicon alloys of about 6 mm initial thickness to a final H-19 condition required for further forming operations, involves the deformation of the material by cold-rolling to about 0.35 mm thickness in four passes before heat-treating the alloy at about 653 K to a fully annealed condition. Thus, the deformation process is continued to a final thickness of approximately 0.03 mm, until a H-19 condition is achieved. The intermediate annealing step of the cold-rolled strip usually involves a preliminary heating stage of about 8-10 hours required to reach the annealing temperature where the alloy is maintained for about 2 more hours before cooling to room temperature. However, despite the very high degree of internal energy provided by the pronounced deformation applied to the material before annealing, precipitation reactions are likely to occur during the early stages of annealing, which would hinder the recrystallization of the material processed, with serious consequences for further manufacturing steps. One of the most remarkable aspects of TRC commercial aluminum alloys is that, as a consequence of the elevated cooling rates involved in the manufacture of these materials, most of the alloying elements are present in a supersaturated solid solution (1-3). The present investigation has been conducted in order to study the recrystallization and restoration kinetics and the

interaction between recrystallization, decomposition of the supersaturated solid solution and precipitation of dispersoids in a commercial TRC Al-Fe-Si alloy employed in the manufacture of household foil and other products for domestic and industrial applications, during annealing after rolling under cold working conditions.

### Experimental techniques

The present investigation has been conducted on samples of a commercial TRC Al-0.56% Fe-0.40% Si alloy whose chemical analysis is presented in Table I.

Table I. Chemical composition of the experimental alloy, wt %.

Fe	Si	Mn	Zn	Cr	Cu	Al
0.56	0.40	0.01	0.004	0.003	0.01	REM

The material has been produced by C.V.G. ALUMINIO DEL CARONI S.A.-DIVISION GUACARA and was provided in the as-cast condition in the form of strip of about 6 mm thickness and 1400 mm width. This initial material was thoroughly characterized by means of optical and electron microscopy techniques as well as tensile and hardness testing conducted on samples machined from the as-cast strip. Small rolling samples of about 300x80x6 mm were also cut from the as-cast strip maintaining the longest edge parallel to the casting direction. Such samples were then cold rolled in a fully instrumented experimental rolling mill to 50% thickness reduction at a peripheral roll speed of about 0.04 ms<sup>-1</sup> using a pair of rolls of 175 mm diameter approximately. The deformed samples were also characterized both from the microstructural and mechanical point of view. Tensile, hardness and other samples for microstructural analysis were also machined from the rolled strips that were subsequently annealed in a salt bath furnace during different time periods in order to follow the microstructural evolution of the material and the changes in the mechanical properties with annealing time. Such treatments were conducted at temperatures of 598, 623, 648 and 673 K for different time intervals ranging between 10 and 50000 s following water quenching to retain the high temperature microstructure. Metallographic samples corresponding to the section defined by the short transverse and rolling directions of the strip were mounted and prepared following a standard metallographic procedure before anodizing in a solution of 52 ml HF (48%) and 973 ml distilled water employing a stainless steel cathode, for their observation under cross polarizers. Scanning electron microscopy analyses were conducted on a HITACHI S-2400 microscope equipped with a KEVEX IV EDX detector, using a constant potential of 20 KV. Transmission electron microscopy studies were carried out on a HITACHI HU-12 microscope using a constant potential of 125 KV. Diffraction patterns were obtained to determine the crystalline structure of the observed phases, employing a camera length of 660 mm. Tensile tests were conducted on a standard universal testing machine with specimens prepared according to the ASTM E8 standard. Testing was carried out at a constant crosshead speed of 0.167 mm s<sup>-1</sup> and a load range of 0-2000 Kg. Vickers hardness tests were performed on previously conditioned samples using a standard equipment with an applied load of 3 Kg. Tensile results represent a mean value of at least three tests for every condition, whereas hardness measurements correspond to the mean value of at least ten measurements.

## Experimental results and discussion

In relation to the metallographic structure of the as-cast material it has been observed that it is mainly composed of elongated grains oriented to an angle of approximately  $45^\circ$  with the direction of casting, possibly as a consequence of the strong shear component of the deformation mode associated to the sticking friction conditions that occur during TRC processes (2,3). As shown in Fig. 1a, the analysis by means of SEM techniques revealed the presence of large second phase particles distributed in the matrix and on the grain boundaries.

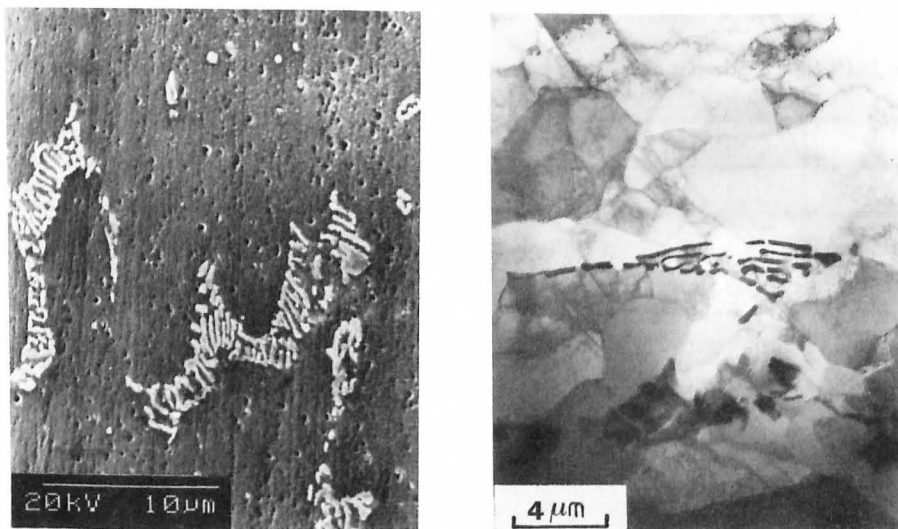


Fig. 1. (a) SEM micrograph of the as-cast structure of the alloy showing typical dendrite-like morphology particles. (b) TEM micrograph of the as-cast material showing particles and dislocations arrangements.

Such particles were observed to present irregular shapes with a dendrite-like morphology, combined also with smaller and more equiaxed particles. EDX analyses carried out on such secondary phases determined that they were composed of Al, Fe and Si and that therefore they could correspond to any of the  $\alpha$  cubic,  $\alpha'$  hexagonal,  $\alpha''$  cubic,  $\alpha_T$  cubic or monoclinic, or  $\beta$  monoclinic AlFeSi phases, according to casting speeds involved and the characteristic morphology above described. TEM analyses of the as-cast samples (Fig. 1b) revealed the presence of a well formed cell structure and dislocations arrangements associated in some areas with primary particles of the type above mentioned. In all the samples that were analyzed finely disperse particles of different sizes were observed, ranging between 0.5 and 1  $\mu\text{m}$ , some of them associated with grain boundaries. By means of microdiffraction patterns taken in some of the particles it was possible to determine that they corresponded to the  $\alpha'$ -AlFeSi hexagonal phase, and the measurements of the lattice parameters conducted on such particles were found to agree reasonably well with the values previously reported (5). In spite of the Fe content of the alloy and according to the casting conditions, it would be expected the presence of  $\text{Al}_m\text{Fe}$  particles. However, such phases were not observed probably due to the fact that the excess

silicon present in the alloy according to the peritectic reaction associates with iron to form the  $\alpha'$ -AlFeSi hexagonal phase which probably corresponds to the equilibrium phase of the system.

### Hardness and tensile stress restoration kinetics

In relation to the change of Vickers hardness and tensile stress with annealing time in the annealing temperature range explored, it has been observed that the mechanical properties tend to achieve a final constant value independent of the annealing time, with the noticeable exception of the samples treated at 598 K. The restoration kinetics has been followed by defining a restoration index of each mechanical property, based on the model of equal strain distribution between the "hard" (deformed) and "soft" (restored) constituents of a massive two-phase alloy, which is based on the linear law of mixtures employed in the determination of the mechanical strength of fiber-reinforced composites. Such an index could be defined readily from the following relationship:

$$P_i = P_0 (1 - X_r) + P_f X_r \quad (1)$$

where  $P_0$  represents the initial value of the mechanical property of the deformed sample without any heat treatment and which constitutes the maximum value of such a property,  $P_f$  the final value corresponding to the fully restored specimen,  $P_i$  the instantaneous value of the property for any intermediate annealing time and  $X_r$  the restoration index or fraction restored. As shown in Fig. 2, the curves corresponding to the change in the index so defined for Vickers hardness as a function of annealing time present a pseudo-sigmoidal aspect characteristic of nucleation and growth processes, although it is understood that all the restoration curves involve both recovery and recrystallization phenomena. In relation to this figure it can be observed that below 623 K the behavior of the material differs appreciably in comparison with the curves at higher annealing temperatures, particularly for restored fractions above 0.7 approximately. In fact, if a JMAK type equation of the form:

$$X_r = 1 - \exp(-kt^n) \quad (2)$$

is used to describe the experimental data at temperatures between 623 and 673 K, JMAK exponents ranging between 0.64 and 0.69 are found with a very high degree of correlation. However, for the data at 598 K the curve even cannot be described by eqn. (2) since after the achievement of restored fractions of the order of 0.7, a shift of the curve towards longer annealing times takes place. This phenomenon could probably be related to the combined action of marked precipitation reactions and recovery effects that occur before the material can achieve a fully restored condition. Therefore, under these circumstances the restoration behavior had to be described by means of a convolution or integration of two JMAK equations which results in an expression of the form:

$$X_r = 1 - f_1 \exp(-K_1 t^{n_1}) - (1 - f_1) \exp(-K_2 t^{n_2}) \quad (3)$$

The five different constants that appear in the above equation were determined by means of a

least square non-linear regression analysis model applied to the experimental values of the restoration index. It has been determined that in this particular case  $K_1 = 2.20 \times 10^{-2}$ ,  $K_2 = 1.02 \times 10^{-4}$ ,  $n_1 = 0.65$ ,  $n_2 = 0.89$  and  $f_1 = 0.72$ . In order to determine the apparent activation energy of the restoration process it is possible to define a normalized restoration time,  $t'$ , that would avoid the need of choosing a particular and arbitrary restored fraction to calculate such an energy.

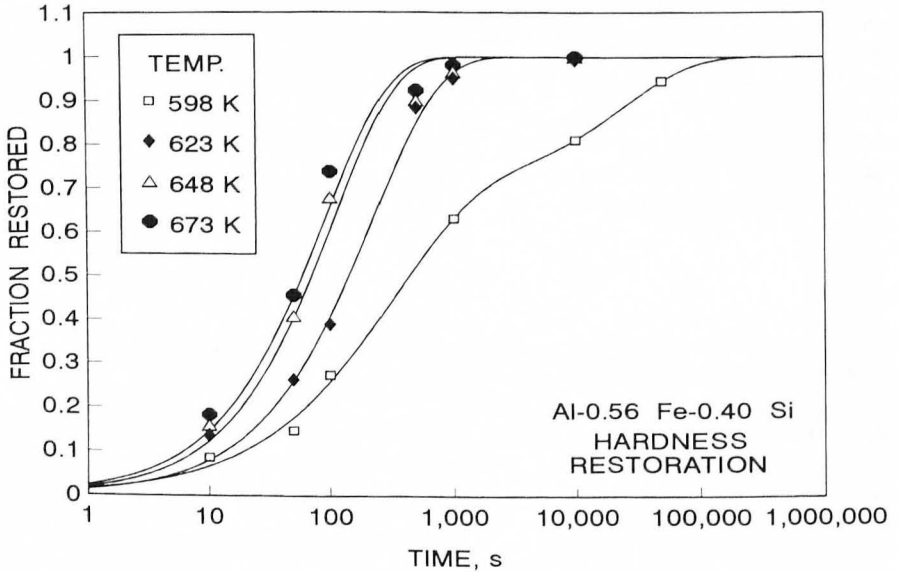


Fig. 2. Change of the fraction restored determined from hardness measurements, with annealing time for different annealing temperatures.

This normalized restoration time can be expressed as:

$$t' = \frac{t_{X_r}}{\left\{ \ln \left[ \frac{1}{1 - X_r} \right] \right\}^{(1/\bar{n})}} \quad (4)$$

where  $t_{X_r}$  represents the time to achieve a particular fraction restored  $X_r$ , and  $\bar{n}$  the mean value of the JMAK exponents previously determined of about 0.66. This normalized restoration time can be expressed as a function of the annealing temperature through a Arrhenius relationship:

$$t' = A \exp \left( \frac{Q}{RT} \right) \quad (5)$$

where  $A$  represents a pre-exponential factor,  $R$  the universal gas constant and  $Q$  the activation energy for restoration. Fig. 3 illustrates the graphical representation of such a relationship where it can be observed that the activation energy for the restoration process or processes

determined from hardness measurements was found to be about  $79.1 \text{ KJmol}^{-1}$ . However, it is important to point out that although this approach can be used confidently in the temperature range 623-673 K, as shown above, it cannot be extrapolated directly for the description of the restoration behavior at lower temperature due to the significant dispersion of the data where possible precipitation effects invalidate the procedure employed at higher temperatures. Such results show that at 598 K the hardness restoration behavior involves quite different processes where the apparent activation energy increases markedly as restoration proceeds.

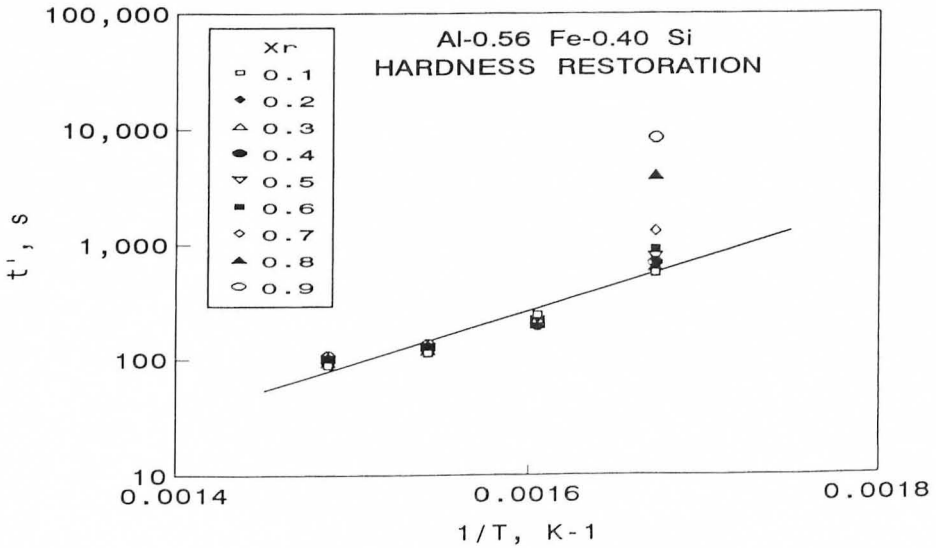


Fig. 3. Temperature-dependence of the normalized time required to achieve different fractions restored.

As it can be observed, the value of  $Q$  determined is significantly lower than the value of the activation energy for self-diffusion usually accepted for commercial aluminum alloys of about  $156 \text{ KJmol}^{-1}$ .

#### Microstructural changes during annealing

The microstructural evolution of the material during annealing at temperatures of 598, 623, 648 and 673 K, from the initial deformed sample until the matrix has been replaced for a partial or a fully recrystallized structure allowed to show that after cold deformation the microstructure developed in the strip is quite inhomogeneous, with the presence of a much coarser grain structure towards the edges of the sample than to the center line. It is believed that nearer the edges of the TRC material the solute supersaturation of the matrix could be quite significant and therefore both solid solution effects and precipitation of small dispersoids could be much more pronounced, leading to a slower recrystallization kinetics and coarsening of the recrystallized grain structure. The observation of the deformed and annealed samples under the optical microscope allowed to determine the time required for the initiation of the recrystallization process. Thus, it has been possible to correct the restoration curve for

recovery effects in order to obtain an approximate recrystallization curve by means of a similar relationship to eqn. (2). From the analyses of these curves it could be observed again that at temperatures below 623 K the recrystallization of the material is severely retarded and that at 598 K the recrystallization process has not been completed even after 50000 s of annealing time, a fact that has been confirmed by means of optical and electron microscopy observations. The SEM analyses of the deformed and partially recrystallized samples revealed that in relation to the morphology of the phases there is a marked tendency of both the dendrite-like and fragmented particles to coarsen or coalesce. On the other hand, the TEM studies conducted on different deformed and annealed samples allowed to determine the presence of a number of small second-phase particles of different sizes ranging between 0.05-0.1  $\mu\text{m}$  approximately, as shown in Fig. 4, although at lower annealing temperatures the number of particles observed per unit area was significantly higher.

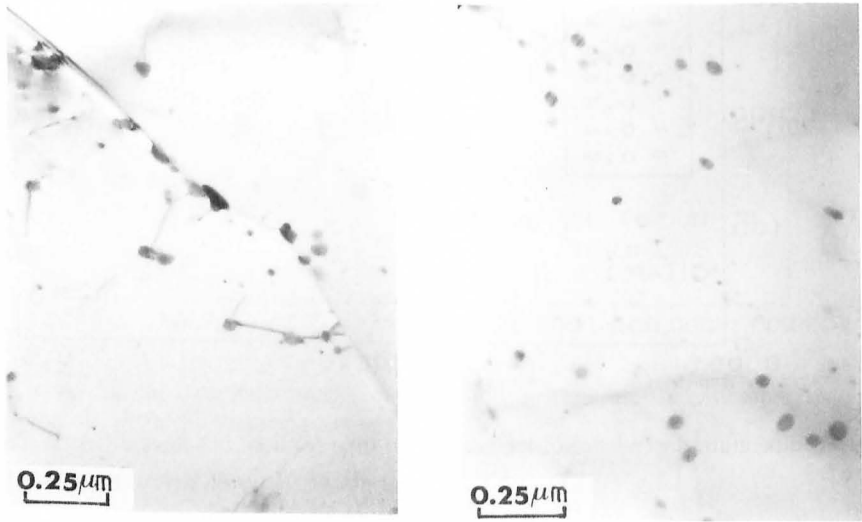


Fig. 4. TEM micrographs corresponding to the sample annealed at 598 K for 50000 s.

Such particles were found to be mostly round in shape although a few elongated phases were also present. Thus, it becomes apparent that during annealing at 598 K precipitation reactions give rise to a massive presence of very small dispersoids that certainly will hinder the restoration and recrystallization behavior of the material, leading to a much coarser final microstructure. It was also determined that there is a clear interaction between such particles and the grain boundaries of the matrix which could severely hinder high angle grain boundary migration during annealing and therefore the nucleation and growth of new recrystallized grains. The crystalline structure of the precipitates was analyzed by means of electron diffraction patterns obtained from some particles suitable in size for this purpose. From lattice parameter measurements conducted on such patterns it was determined that the small dispersoids also corresponded to the  $\alpha'$ -AlFeSi hexagonal phase.

## Conclusions

In the temperature range investigated it is possible to differentiate two distinct intervals where the restoration of the mechanical properties presents different behaviors. At temperatures lower than 623 K there is evidence that the restoration and recrystallization behavior of the material is hindered by precipitation of small dispersoids mostly of the type  $\alpha'$ -AlFeSi hexagonal phase. Under these circumstances it is not possible to determine a characteristic value of the apparent activation energy for the operating process or processes since as they proceed there is an apparent continuous increment of such a parameter. At temperatures above 623 K, the restoration and recrystallization behavior of the material occur continuously following a smooth sigmoidal curve. The activation energy determined in the temperature range of 623-673 K for restoration of hardness was found to be approximately  $79.1 \text{ KJmol}^{-1}$ . Also, it has been determined that the strain applied to the material plays an important role in the coarsening of large dendrite-like morphology second-phase particles during subsequent annealing stages which at industrial level occur at relatively low temperatures (below 673 K).

## References

1. E. Nes, Microstructural Control in Aluminum Alloys: Deformation, Recovery and Recrystallization, Eds. E. Chia and H.J. McQueen, (TMS-AIME, Warrendale, Pa, USA, 1986), pp. 179-196.
2. J. Strid, Proc. 3rd Internat. Conf. on Aluminium Alloys, Eds. L. Arnberg, O. Lohne, E. Nes and N. Ryum, (Norwegian Institute of Technology, Trondheim, Norway, vol. III, 1992), pp. 321-356.
3. J. Strid, 2nd. International School on Aluminium Alloy Technology, (The Norwegian Institute of Technology, University of Trondheim, Norway, 1993).
4. P. Skjerpe, Met. Trans., **18A**, 1987, pp.189-200.

## Acknowledgments

The present investigation has been carried out with the financial support of the Venezuelan National Council for Scientific and Technological Research (CONICIT) through the projects S1-2580 and RP-II-C-135, and the financial support of the Scientific and Humanistic Development Council of the Central University of Venezuela. The assistance of Mrs. Sonia Camero and Mrs. Joslinda Arraiz in the electron microscopy studies is gratefully acknowledged. C. Villalobos and A. Piñeiro also acknowledge the bursary given to them by C.V.G. ALUMINIO DEL CARONI S.A. -DIVISION GUACARA and FUNDACION "GRAN MARISCAL DE AYACUCHO" during the conduction of the present investigation.